Published in final edited form as:
Metabolism. 2011 August ; 60(8): 1070–1080. doi:10.1016/j.metabol.2010.11.003.

Short-term hyperglycemia increases arterial superoxide production and iron dysregulation in atherosclerotic monkeys

Patrick A. Rowe, **Kylie Kavanagh**, **Li Zhang**, **H. James Harwood Jr.**, and **Janice D. Wagner**
Department of Pathology, Wake Forest University Health Sciences, Winston-Salem, NC, 27157, USA

Abstract

Objective—The incidence and severity of atherosclerotic vascular disease is increased in diabetics, in part due to increased production of reactive oxygen species (ROS). Previously we found both increased atherosclerosis and arterial protein oxidation six months after streptozotocin-induced diabetes in monkeys fed an atherogenic diet, the pattern of which was indicative of redox-active transition metal involvement. The goal of this study was to determine if short-term (one month) hyperglycemia increases oxidative stress and dysregulates iron metabolism prior to differences in atherosclerosis.

Methods—Cynomolgus monkeys with pre-existing atherosclerosis were stratified by dietary history and plasma lipids and received either streptozotocin (STZ-DM; n=10) or vehicle (control; n=10). One month after diabetes induction, blood and artery samples were collected.

Results—There were no differences in plasma lipoprotein cholesterol, arterial cholesterol, and atherosclerosis between control and STZ-DM. However, plasma lipid peroxides were elevated 137% ($p<0.01$), arterial superoxide was increased 47% ($p<0.05$), plasma ferritin, an indicator of whole-body iron stores, was 46% higher ($p<0.05$), and iron deposition within aortic atherosclerotic lesions was more prevalent in STZ-DM compared to controls. Arterial levels of the antioxidant enzymes, superoxide dismutase, catalase, and heme oxygenase-1 were not higher in STZ-DM, even though superoxide was higher, suggesting impaired antioxidant response.

Conclusions—The increase in ROS prior to differences in atherosclerosis supports ROS as an initiating event in diabetic vascular disease. Further studies are needed to determine if increases in iron stores and arterial iron deposition promotes hydroxyl radical formation from superoxide and accelerates diabetic vascular damage.

Correspondence to: Janice D. Wagner, DVM, Ph.D., Wake Forest University School of Medicine, Department of Pathology, Comparative Medicine Clinical Research Center, Medical Center Boulevard, Winston-Salem, NC 27157-1040; Ph (336) 716-1630; FAX (336) 716-1501; jwagner@wfubmc.edu.

Disclosure Statement: No potential conflicts of interest exist with any of the authors of this manuscript.

AUTHOR CONTRIBUTIONS

Patrick A. Rowe - study design, conduction of study, data collection, data analysis and interpretation, manuscript writing
Kylie Kavanagh - study design, data collection, data analysis
Li Zhang - data collection, data analysis
H. James Harwood Jr. - data interpretation, manuscript writing
Janice D. Wagner - study design, data interpretation, manuscript writing

Keywords

Oxidative stress; reactive oxygen species; ferritin; diabetic vascular disease

INTRODUCTION

Cardiovascular disease, the primary cause of death among diabetic patients, occurs at an earlier age and results in two-fold to eight-fold greater mortality rates than in nondiabetic patients [1]. The primary cause of this increased incidence of vascular disease, which includes cerebrovascular disease, coronary heart disease, and peripheral vascular disease, is atherosclerosis [2,3]. Although the exact mechanisms responsible for the increase in atherosclerosis are unclear, epidemiologic evidence suggests that only 25% of the excess coronary heart disease in diabetics can be accounted for by changes in traditional risk factors such as hypercholesterolemia, hypertriglyceridemia, hypertension, and obesity [3,4], suggesting that the increased vascular disease may involve factors unique to the diabetic patient.

Chronic hyperglycemia, a common feature of all forms of diabetes, contributes significantly to both the microvascular and macrovascular complications of the disease and has been linked to the increased incidence of atherosclerosis in diabetic patients [5,6], suggesting that glucose itself may be toxic to the vasculature [4]. Indeed, the United Kingdom Prospective Diabetes Study demonstrated that strict glycemic control dramatically lowered the incidence of microvascular diseases (retinopathy, nephropathy, and neuropathy) and a 10-year follow-up showed an emergent risk reduction for myocardial infarction for subjects receiving intensive glucose-lowering therapy during the trial [4,7]. Furthermore, it has been suggested that vascular endothelial cells and mesangial cells are particularly sensitive to the damaging effects of hyperglycemia since they are relatively inefficient in their ability to prevent glucose transport in response to hyperglycemia, resulting in high intracellular glucose levels [8].

Oxidative stress has been postulated as a major contributor to both microvascular and macrovascular diabetic complications and it has been suggested that many, if not all of the mechanisms that relate hyperglycemia to vascular disease involve the overproduction of reactive oxygen species (ROS) [4,9,10]. A consistent differentiating feature common to all cell types that are damaged by hyperglycemia is an increased production of ROS, in particular, the overproduction of superoxide [4,8,11–13]. In fact, it has been proposed that the overproduction of superoxide that occurs in response to mitochondrial dysfunction in diabetes, is the unifying mechanism by which hyperglycemia exerts its role in producing vascular damage [4,8,14].

It is unlikely that superoxide per se, is the ROS that is directly responsible for all of the vascular damage, since it has a relatively limited reactivity with biomolecules [15]. Superoxide is, however, readily converted to more reactive species such as the hydroxyl radical, through the actions of superoxide dismutase (SOD) and transition metal-catalyzed Fenton reactions (Eqns. 1 & 2), and peroxynitrate, through its reaction with endothelial cell-derived nitric oxide [4,16,17].

$$\text{SOD reaction} \quad 2O_2^{\cdot -} + 2H^+ \rightarrow H_2O_2 + O_2 \quad (1)$$

$$\text{Fenton reaction} \quad H_2O_2 + Fe^{2+} \rightarrow {}^{\cdot}OH + {}^{-}OH + Fe^{3} \quad (2)$$

Studies in streptozotocin-induced diabetic (STZ-DM) monkeys have suggested that hydroxyl radical is responsible for hyperglycemia-induced vascular damage [16]. Considered the most destructive ROS in nature [18–21], hydroxyl radicals rapidly react with most biomolecules [22,23]. However, since they are short-lived and diffuse only a finite distance before reacting, hydroxyl radicals must be produced within the vasculature in order to exert damage there.

The development of diabetes has been shown to be associated with an increase in whole body iron stores, with reports of elevated serum ferritin not only in type 2 diabetic patients but also in insulin-resistant nondiabetic individuals [24–27]. In addition, there is considerable evidence that increases in whole body iron stores, such as those in patients with familial hemochromatosis, also predisposes to insulin resistance and diabetes [24] and that repetitive phlebotomy and/or iron chelation therapy using agents such as deferoxamine not only reduce ferritin levels in these patients but also improve insulin sensitivity and glycemic control [24].

However, as these studies are primarily associative in nature it has been difficult to determine whether hyperglycemia per se increases whole body iron stores and, if so, the time-frame in which this may occur. Evidence argues against a generalized increase in oxidative stress in diabetes but rather supports localized generation of ROS species within microenvironments of the vasculature [4]; the role of iron in the ROS-mediated vascular damage induced by hyperglycemia in diabetes is appealing. Unfortunately, information on the role of oxidative damage and its relationship to vascular dysfunction and atherosclerosis in diabetic humans is limited. This is in part the result of both dietary variations within the human population and variability in dietary and supplemental intake of vitamins and minerals that may either have antioxidant properties or modify iron metabolism.

To study early oxidative events in the development of diabetes, we conducted studies examining ROS production, iron deposition, and atherosclerosis in vascular tissue of monkeys fed a standardized western-type diet in which diabetes was induced with streptozotocin [16, 28–30]. In previous studies using this model, we demonstrated that six months of hyperglycemia resulted in both an increase in atherosclerosis extent [29] and arterial oxidation [16]. Unfortunately, as oxidative stress and atherosclerosis increased concomitantly at this time-point, we could not determine whether the oxidation preceded, and possibly contributed to the hyperglycemia-induced atherosclerosis development or occurred as a consequence of the increased atherosclerosis.

In the present study, we assessed differences in systemic and arterial ROS production as well as iron deposition within the vasculature after a shorter, one month period of hyperglycemia in STZ-DM monkeys, a time at which treatment-induced differences in atherosclerosis development was not anticipated and therefore would not confound interpretation.

METHODS

Animals

All monkeys were fed a moderately atherogenic diet containing 0.18 mg of cholesterol/Kcal with 35% of calories from fat, for a minimum of three months prior to induction of diabetes and throughout the 1-month study period. Prior to this study, monkeys had been fed variable experimental diets, accounted for by calculating historical dietary cholesterol exposure (mg cholesterol/calorie in diet x number of days fed diet). Monkeys were stratified into control (n = 10) and STZ-DM (n = 10) groups by their dietary cholesterol history and their pretreatment plasma total cholesterol to high-density lipoprotein cholesterol (HDLC) ratio to

balance atherosclerosis risk at baseline [29]. All animal procedures performed during this study were done in accordance with the Institutional Animal Care and Use Committee of the Wake Forest University School of Medicine.

Induction of Diabetes Mellitus

Diabetes was induced with streptozotocin (Zanosar, Upjohn, Kalamazoo, MI) as previously described [28–30]. Seven of the ten monkeys became diabetic (fasting blood glucose >126 mg/dL) three days after streptozotocin treatment. The remaining three monkeys received two additional doses of streptozotocin to induce diabetes. STZ-DM monkeys were maintained on Novolin 70/30 insulin (Novo Nordisk USA, Princeton, NJ) to mimic moderately controlled diabetes in humans (8–10% glycated hemoglobin, HbA_{1c}). Seven days after diabetes induction, intravenous glucose tolerance tests (IVGTT) were performed to assess beta cell responses to glucose challenge. Parameters measured included area-under-the-curve for glucose and insulin, as well as K-values for glucose disappearance rate [28].

Sample Collection

Monkeys were sedated with ketamine (10–15 mg/kg IM) after an 18-hour fast for blood sampling at baseline and 4 weeks. Serum, plasma and whole blood samples were stored at −80°C. At study end, monkeys were sedated, and then anesthetized with sodium pentobarbital (80 mg/kg body wt IV) before exsanguination and collection of heart, aorta, and arteries.

Clinical Chemistry Analyses

Total plasma cholesterol, triglycerides, apolipoprotein B (apoB) cholesterol [low-density lipoprotein (LDL) + very low-density lipoprotein (VLDL) cholesterol], and HDLC were measured [29–31]. Plasma free fatty acids were measured by colorimetric assay (Wako Chemicals USA, Richmond, VA). Plasma glucose concentrations were determined by the glucose oxidase method (Roche Diagnostics, Indianapolis, IN), fructosamine concentrations by the Nitro Blue colorimetric methodology (Roche Diagnostics, Indianapolis, IN), and HbA_{1c} by automated affinity HPLC (Primus, Kansas City, MO) as described [16,30,31]. Insulin and C-peptide were determined by ELISA (Mercodia, Uppsala, Sweden). Plasma lipid peroxides were measured by colorimetric assay (Zeptometrix, Buffalo, NY) and plasma oxidized LDL (oxLDL) concentrations determined by an ELISA that detects oxidized apoB antigen (Mercodia, Uppsala, Sweden). Plasma ferritin concentrations were determined by ELISA (AssayPro, St. Charles, MO) and serum iron was measured using an Alfa Wassermann ACE analyzer (direct TIBC, Reference Diagnostics Inc., Bedford, MA).

Arterial Superoxide Levels

Lucigenin-enhanced chemiluminescence provided relative measures of superoxide levels [32]. Segments of carotid arteries were placed into microtiter plate wells containing phosphate-buffered saline with and without 1 mM NADPH. The arteries were maintained at 37°C for 30 minutes and then scintillation counts obtained for 20 minutes in the presence of lucigenin [9,9′-bis(*N*-methylacridinium nitrate), 5 μmol/L] (Sigma-Aldrich, St. Louis, MO) using a Fluostar Optima luminometer (BMG Labtech, Durham, NC). Background-corrected values were normalized to dry tissue weight (μg) and reported as either basal counts or NADPH-stimulated counts to basal counts.

Superoxide levels were also assessed by formation of 2-hydroxyethidium, modified from methodology based on the conversion of dihydroethidine (DHE) to 2-hydroxyethidium in the presence of superoxide [33]. A 1 cm segment taken near the abdominal /thoracic aorta

junction was placed into ice cold Krebs-HEPES buffer (KHB) and cut into thin rings (~2 mm). Rings were placed into wells with KHB containing 10 μM DHE (Invitrogen, Carlsbad, CA), incubated at 37°C in 95% air/ 5% CO_2 for 20 minutes, washed with KHB, then incubated for 1 hour before transferring to methanol (1:10 w/v), and stored for analysis at −80°C. Prior to analysis, tissues were homogenized and supernatant retained for HPLC determination with a C-18 reverse phase column (Nucleosil 250, 4.5 mm; Sigma-Aldrich, St. Louis, MO) equipped with UV and fluorescence detectors. The mobile phase consisted of 1% trifluoroacetic acid with increasing acetonitrile concentration (10–70%) (Alltech SelectPro fluid processor, Alltech, Deerfield, IL, USA) over 50 minutes at a flow rate of 0.5 mL/minute to separate DHE, ethidium, and 2-hydroxyethidium. Formation of 2-hydroxyethidium was monitored with the fluorescence detector (em 580 ex 480 nm) and DHE was detected by UV absorption at 355 nm.

Arterial Cholesterol and Lipid Peroxides

A segment of carotid artery was removed and snap frozen in liquid nitrogen. Chloroform - methanol lipid extracts were prepared and total and free cholesterol concentrations were determined enzymatically [29]. Esterified cholesterol was calculated as the difference between total and free cholesterol. Arterial lipid peroxide concentrations were measured in the same lipid extracts used for cholesterol determinations [30], and expressed as malondialdehyde equivalents.

Aortic Iron and Atherosclerotic Lesion Area

Sections of thoracic aorta were placed for 1 h at 37°C in Perl's solution containing 7% potassium ferrocyanide and 3% hydrochloric acid to stain ferric iron (Fe^{3+}). The sections were then incubated in 0.75 mg/mL diaminobenzidine for 15 minutes, followed by 15 minute incubation with 0.015 % hydrogen peroxide. Perl's iron staining was graded by a blinded assessor on a 0, 1, 2, 3 scale, using photomicrographs assembled from high-magnification digital images using ImagePro Plus 5.1 (Media Cybernetics, Bethesda, MD). Sections were subsequently analyzed to determine atherosclerotic lesion area. The intimal (lesion) area (mm^2) was determined by subtracting lumen area from total area within the internal elastic lamina.

Immunoblotting

Frozen abdominal aorta was ground with a mortar and pestle in liquid nitrogen into a fine powder, prior to protein extraction, gel electrophoreses and transfer to nitrocellulose membranes as previously described [34]. The membranes were probed with antibodies to the various SODs [manganese SOD (MnSOD), copper/zinc SOD (Cu/ZnSOD), and extracellular SOD (EcSOD)] (Nventa Biopharmaceuticals, San Diego, CA), heme oxygenase-1 (Nventa Biopharmaceuticals, San Diego, CA), and catalase (EMD Chemicals, San Diego, CA). After labeling the membranes with the appropriate horseradish peroxidase-conjugated secondary antibody, they were developed using an ECL-plus detection reagent (GE Healthcare, Giles, UK) and quantified by expressing their respective densities as arbitrary units (AU) normalized to β-actin bands [34].

Statistical Analysis

Values are presented as means ± SEM. Measures which were not normally distributed were log transformed to satisfy the normality assumption. Group differences were determined using Student's t-test or ANCOVA (if baseline measures available as covariates. Baseline plasma lipid peroxide concentrations were used as covariates for arterial superoxide measures as they significantly predicted the outcome measures. Differences between proportions of positive arterial Perls staining were assessed by the chi-square statistic.

Significance was set at $p < 0.05$. Analyses were done using SAS v9.1.3 (SAS Institute, Cary, NC).

RESULTS

Experimental Diabetes Induction

There were no significant differences between the control and STZ-DM groups with respect to age (17 ± 2 years versus 12 ± 2 years respectively; p = 0.10), body weight (6.8 ± 0.7 kg versus 6.0 ± 0.4 kg respectively; p = 0.30), plasma total cholesterol (252 ± 17 mg/dL versus 301 ± 43 mg/dL respectively; p=0.28), triglycerides (33 ± 5 mg/dL versus 49 ± 9 mg/dL respectively; p=0.12) and glycemic measures at baseline (Table 1). IVGTT performed 7 days after induction confirmed that STZ-DM monkeys had significantly reduced ability to clear glucose and secrete insulin (both *p's* < 0.001; Fig 1), indicative of beta cell destruction. As expected, plasma glucose, fructosamine, and HbA_{1c} levels were significantly higher in STZ-DM compared to control monkeys (Table 1). Plasma insulin and C-peptide concentrations were lower in STZ-DM compared to control monkeys (Table 1).

Plasma and Arterial Lipids

One month after induction, there were no differences in total cholesterol, apoB cholesterol, HDLC, or free fatty acid concentrations between STZ-DM and control monkeys (Table 2). Furthermore, there were no differences in carotid artery total cholesterol, free cholesterol, or esterified cholesterol, and no differences in aortic intimal area between the STZ-DM and control monkeys (Table 2), consistent with the short time-frame after diabetes induction. Plasma triglycerides were significantly increased in STZ-DM monkeys.

Plasma Oxidation Measures

Plasma lipid peroxides were similar between STZ-DM and control groups at baseline (9.3 ± 1.0 nmol/mL versus 7.8 ± 0.6 nmol/mL, respectively), but increased 137% from baseline ($p < 0.01$) in STZ-DM compared to 7% decrease from baseline in control monkeys (Fig. 2A). Similarly, oxLDL concentrations increased 67% from baseline (p = 0.08) in STZ-DM monkeys compared to a 6% reduction from baseline in control monkeys (Fig. 2A).

One month after diabetes induction, plasma ferritin concentrations were significantly higher in STZ-DM than in control monkeys ($p < 0.05$). Serum iron levels also tended to be higher (p=0.08) but just failed to reach statistical significance (Fig. 2B).

Aortic Iron Deposition

Iron deposition within atherosclerotic lesions is thought to contribute to the oxidative stress common to the atherosclerotic lesion [35]. Perl's staining of thoracic aortic segments revealed ferric iron deposits in thoracic aortas from both control (Fig. 3A) and STZ-DM monkeys (Fig. 3B). Iron staining was considerably more prevalent in STZ-DM than control monkeys ($p < 0.05$).

The two representative aortic sections shown in Fig. 3 were chosen because they have comparable atherosclerotic lesion areas. To assess the relationship between iron deposits and lesion area among STZ-DM and control monkeys, we compared the atherosclerotic lesion size and grade of Perl's staining for each arterial section. There was no relationship apparent between lesion size and iron staining in either control or STZ-DM monkeys (Fig. 4). This suggests that increased iron deposition in STZ-DM arteries was not a consequence of atherosclerotic lesion development, but rather a consequence of diabetes.

Arterial Superoxide production

Arterial superoxide levels were higher in STZ-DM monkeys as determined using two different methodologies (Fig. 5). Basal superoxide levels determined by 2-hydroxyethidium formation were 47% greater ($p < 0.05$) in aortae from STZ-DM compared to control monkeys (Fig. 5A). In carotid artery, basal superoxide levels determined by lucigenin-enhanced chemiluminescence were not significantly different ($p = 0.66$) between STZ-DM (2822 ± 647 arbitrary units/mg tissue) and control monkeys (3265 ± 745 arbitrary units/mg tissue), but were 56% greater ($p = 0.04$) in STZ-DM compared to control monkeys after stimulation with NADPH (Fig. 5B), suggestive of the involvement of the phagocyte NADPH oxidase.

Vascular Antioxidant Enzyme Levels

In normal vascular tissues, antioxidant enzymes that degrade superoxide (Cu/ZnSOD, EcSOD, MnSOD), hydrogen peroxide (catalase), and heme (heme oxygenase-1) are elevated in response to increased oxidative stress in order to decrease tissue levels of ROS [4,24]. However, protein levels of the SODs, catalase, and heme oxygenase-1 were not elevated in the aortas of STZ-DM monkeys when compared to the aortas of control animals (Table 3), even though plasma lipid peroxides (Table 2) and arterial superoxide levels (Fig. 5) were significantly elevated.

DISCUSSION

Diabetes mellitus increases the incidence, severity, and mortality [1,36–38] of coronary artery disease independently from other traditional risk factors. Plasma markers of oxidant stress are increased in diabetic patients [39,40] and participate in progression of vascular disease [4,11,41,42]. However, as ROS production increases with atherosclerosis development, it is hard to determine whether the increased ROS is causative or coincident with the increased vascular disease in diabetes. Here we show that increases in systemic and arterial ROS production occur prior to development of increased atherosclerosis in streptozotocin-induced diabetic monkeys. Further, we found evidence of increased whole body iron stores as well as increased arterial iron deposition in diabetic monkeys that were fed a western diet with controlled amounts of mineral and vitamin content.

The streptozotocin-induced diabetic model induces a hyperglycemic condition with diminished insulin production (Fig. 1). The significant, but incomplete reduction in fasting insulin and C-peptide levels in STZ-DM compared to control monkeys, together with their lack of insulin resistance and negligible insulin responses during IVGTT, is due to marked, albeit incomplete, beta cell loss after streptozotocin treatment [28]. This resembles the residual insulin production observed in humans with type 1 diabetes months or years after onset [43], and contrasts with insulin responses in either humans or cynomolgus monkeys with type 2 diabetes [44], indicating that changes in the pancreatic islets of STZ-DM monkeys are more characteristic of type 1 diabetes than type 2 diabetes [28,44].

In this study we demonstrated that, within one month of hyperglycemia induction, at a time when there were no differences in plasma lipoprotein cholesterol, arterial cholesterol, and atherosclerosis extent between control and STZ-DM monkeys, circulating lipid peroxides and oxLDL were elevated, arterial basal superoxide and NADPH-stimulated superoxide concentrations were higher, plasma ferritin (an indicator of whole-body iron stores) and serum iron were elevated, and iron deposition within atherosclerotic lesions was more prevalent in STZ-DM compared to controls. The increases in ROS, particularly arterial superoxide, observed prior to differences in atherosclerosis are consistent with the hypothesis that elevated ROS production is an initiating event in diabetic vascular disease.

Furthermore, the increase in iron stores and arterial iron deposition that occurred within one month of diabetes induction are also consistent with the suggestion that redox-active iron within the artery may play a role in catalyzing the production of hydroxyl radicals from elevated arterial superoxide, resulting in accelerated diabetic vascular damage.

Several mechanisms may account for the hyperglycemia-induced superoxide production. Hyperglycemia per se has been shown to stimulate mitochondrial superoxide overproduction in endothelial cells *in vitro* [8,14], and *in vivo* studies have suggested the importance of this pathway in vascular dysfunction [45] and atherosclerosis development [46] in diabetic animals. Activation of RAGE may also contribute to vascular superoxide production, as treatment of cultured human umbilical vein endothelial cells with advanced glycation end products have been shown to stimulate superoxide production and subsequent inflammatory gene expression [47].

Another pathway for generating reactive oxidant species involves nitric oxide, which is produced by endothelial cells to regulate vascular tone [6]. Nitric oxide can react with superoxide to produce peroxynitrite, a potent oxidant that can react with protein tyrosine residues to produce 3-nitrotyrosine, which is a marker of the reactive nitrogen pathway [4,6]. However, in previous studies in STZ-DM monkeys we found that levels of 3-nitrotyrosine in arterial proteins were not elevated in STZ-DM monkeys relative to control animals [16], suggesting that hyperglycemia does not increase the production of reactive nitrogen species in artery walls of these diabetic animals.

Vascular macrophages can also generate superoxide and hydrogen peroxide through the action of NADPH oxidase. The hydrogen peroxide can be used by another macrophage enzyme, myeloperoxidase, to produce more potent cytotoxic oxidants, such as hypochlorous acid [4,6]. Indeed, human studies have demonstrated increased NADPH oxidase activity and protein levels in arteries from diabetic patients [48]. The higher arterial superoxide levels from STZ-DM monkeys after stimulation with NADPH also suggest the potential involvement of NADPH oxidase in diabetic vasculature. In our previous studies in STZ-DM monkeys where arterial proteins were isolated, levels of o,o′-dityrosine, a marker of myeloperoxidase activity, were significantly increased, but did not correlate with degree of hyperglycemia [16]. Additional studies using inhibitors of NADPH oxidase, such as apocynin, could help to explore the potential for a role of phagocyte NADPH oxidase versus myeloperoxidase.

It is also interesting that arterial superoxide levels were increased but not the less specific arterial lipid peroxidation (Table 2), suggesting that superoxide production is a specific glucose-induced ROS mechanism. Importantly, protein levels of antioxidant enzymes (SOD, catalase, and heme oxidase) responsible for the conversion of superoxide to less harmful species were unchanged in aortic tissue from STZ-DM monkeys, suggesting that higher superoxide levels equates to higher arterial damage.

Increases in circulating ferritin and iron levels in insulin resistant states such as the metabolic syndrome, gestational diabetes, polycystic ovary syndrome, and familial hemochromatosis, are thought to play a role in increased risk of type 2 diabetes [24]. This concept is supported by the observations that reductions in whole body iron load, through repetitive phlebotomy and/or iron chelation therapy using deferoxamine, results in improvements in insulin sensitivity and glycemic control and reduces the risk of diabetes in patients with familial hemochromatosis [24]. Furthermore, the strong pro-oxidant effects of iron are associated with increased levels of oxidative stress thought to play a role in diabetic vascular complications [24]. Similar to findings in diabetic [25,26] and insulin-resistant nondiabetic people [27], plasma ferritin levels were higher in STZ-DM monkeys (Fig. 2).

Additionally, serum iron concentrations tended to be greater. These measures indicate that whole-body iron stores are likely increased. In addition to these indirect systemic indicators of iron stores, ferric iron deposition was more prevalent in aortic sections from STZ-DM monkeys (Fig. 3,4). The staining pattern appeared to be lumen-associated and non-uniform, suggesting involvement of macrophage-associated hemosiderin. Also, hemoglobin may be the source of this iron, derived either from intravascular hemolysis or erythrocyte attachment to the endothelium via RAGE [49].

It has been proposed that the overproduction of superoxide that occurs in response to mitochondrial dysfunction, may be the unifying mechanism by which hyperglycemia exerts its role in producing vascular damage, via its dismutation to produce hydrogen peroxide, which in the presence of redox-active transition metals, such as iron, produces hydroxyl radicals which act locally within arteries to produce damage [4,8]. As mentioned above, tissue hydroxyl radical production depends directly on both the availability of free iron and the balance between production of hydrogen peroxide, primarily via dismutation of superoxide, and degradation by antioxidant enzymes such as catalase [4]. The increase of both superoxide and iron content in the artery wall would likely lead to increased hydroxyl radical formation [4,17]. This is consistent with our previous study where we found increases in three protein modifications, *ortho*-tyrosine, *meta*-tyrosine and *o,o′*-dityrosine but not 3-nitrotyrosine in aortic tissue of hyperglycemic animals [16]. In these studies, various oxidative agents were tested in arterial samples and only hydroxyl radical mimicked the pattern of oxidized amino acids [16]. Moreover, glycemic control was strongly correlated with the tissue concentration of both *ortho*-tyrosine and *meta*-tyrosine further suggesting that glucose levels were promoting specific oxidative pathways [16].

In summary, the increase in superoxide production in diabetes prior to differences in atherosclerosis suggests that increased ROS is an important initiating event in vascular disease. The increase in whole body iron stores (ferritin and serum iron) and particularly arterial iron in the presence of higher superoxide levels may catalyze production of hydroxyl radicals resulting in vascular damage. Furthermore, in our previous studies [16,17] and in this report, hyperglycemia results in activation of specific pathways of ROS generation, and not in generalized lipid oxidation. A limitation of this study is that the exact mechanisms through which hyperglycemia increases iron stores could not be determined. In this regard, the iron chelator, deferoxamine, an agent used to treat iron overload in humans [50] has been reported to reduce atherosclerosis in both cholesterol-fed rabbits [51] and in C57BL6J mice [52] and to upregulate glucose uptake and insulin signaling in rat liver [53]. Further studies with iron chelation agents, such as deferoxamine, in diabetic monkeys, could provide additional mechanistic insight into the role of iron in the development of diabetic vascular disease.

Acknowledgments

The authors thank Joel Collins, Mickey Flynn, Scott Isom, Samuel Rankin, Aida Sajuthi, and Gina Ward for technical assistance and Drs. Prasad Katakam and David Busija for helpful suggestions during the execution of these studies. This work was completed as partial fulfillment of Dr. Rowe's requirements for the degree of Doctor of Philosophy from Wake Forest University School of Medicine.

SOURCES OF FUNDING

Funding for these studies was from institutional sources including the Elizabeth Perry Skorich Diabetes Research Fund.

LIST OF ABBREVIATIONS

ApoB	apolipoprotein B
AU	arbitrary units
DHE	dihydroethidine
HDLC	high-density lipoprotein cholesterol
IVGTT	intravenous glucose tolerance tests
KHB	Krebs-HEPES buffer
LDL	low-density lipoprotein
oxLDL	oxidized LDL
RAGE	receptor for advanced glycation end products
ROS	reactive oxygen species
SEM	standard error of the mean
SOD	superoxide dismutase
STZ-DM	streptozotocin-induced diabetic
VLDL	very low-density lipoprotein

References

1. Kannel WB, McGee DL. Diabetes and cardiovascular disease. The Framingham study. J Am Med Assn. 1979; 241:2035–2038.
2. Bierman EL. Atherosclerosis in diabetes. Arterioscler Thromb. 1992; 12:647–656. [PubMed: 1591228]
3. Pyorala K, Laakso M, Uusitupa M. Diabetes and atherosclerosis: an epidemic view. Diabetes Metab Rev. 1987; 3:463–524. [PubMed: 3552530]
4. Pennathur S, Heinecke JW. Mechanisms of oxidative stress in diabetes: implications for the pathogenesis of vascular disease and antioxidant therapy. Fronteers Biosci. 2004; 9:565–574.
5. Kuusisto J, Mykkanen L, Pyorala K, et al. NIDDM and its metabolic control predict coronary heart disease in elderly subjects. Diabetes. 1994; 43:960–967. [PubMed: 8039603]
6. Nathan DM, Cleary PA, Backlund JY, Genuth SM, Lachin JM, Orchard TJ, et al. Intensive diabetes treatment and cardiovascular disease in patients with type 1 diabetes. N Engl J Med. 2005; 353:2643–2653. [PubMed: 16371630]
7. Holman RR, Paul SK, Bethel MA, Matthews DR, Neil HAW. 10-Year follow-up of intensive glucose control in type 2 diabetes. N Engl J Med. 2008; 359:1577–1589. [PubMed: 18784090]
8. Brownlee M. The pathogenesis of diabetic complications: a unifying mechanism. Diabetes. 2005; 54:1615–1625. [PubMed: 15919781]
9. Haidara MA, Yassin HZ, Rateb M, Ammar H, Zorkani MA. Role of oxidative stress in development of cardiovascular complications in diabetes mellitus. Curr Vasc Pharmacol. 2006; 4:215–227. [PubMed: 16842139]
10. Nishikawa T, Araki E. Impact of mitochondrial ROS production in the pathogenesis of diabetes mellitus and its complications. Antioxid Redox Signal. 2007; 9:343–353. [PubMed: 17184177]
11. Li JM, Shah AM. Endothelial cell superoxide generation: regulation and relevance for cardiovascular pathophysiology. Am J Physiol Regul Integr Comp Physiol. 2004; 287:R1014–1030. [PubMed: 15475499]
12. Bubolz AH, Li H, Wu Q, Liu Y. Enhanced oxidative stress impairs cAMP-mediated dilation by reducing Kv channel function in small coronary arteries of diabetic rats. Am J Physiol Heart Circ Physiol. 2005; 289:H1873–880. [PubMed: 15937095]

13. Ding H, Hashem M, Triggle C. Increased oxidative stress in the streptozotocin-induced diabetic apoE-deficient mouse: changes in expression of NADPH oxidase subunits and eNOS. Eur J Pharmacol. 2007; 561:121–128. [PubMed: 17292348]
14. Du X, Matsumura T, Edelstein D, et al. Inhibition of GAPDH activity by poly(ADP-ribose) polymerase activates three major pathways of hyperglycemic damage in endothelial cells. J Clin Invest. 2003; 112:1049–1057. [PubMed: 14523042]
15. Bielski BH, Shiue GG. Reaction rates of superoxide radicals with the essential amino acids. Ciba Found Symp. 1978 Jun; 6–8(65):43–56. [PubMed: 22422014]
16. Pennathur S, Wagner JD, Leeuwenburgh C, Litwak KN, Heinecke JW. A hydroxyl radical-like species oxidizes cynomolgus monkey artery wall proteins in early diabetic vascular disease. J Clin Invest. 2001; 107:853–860. [PubMed: 11285304]
17. Monnier VM. Transitional metals redox: reviving an old plot for diabetic vascular disease. J Clin Invest. 2001; 107:799–801. [PubMed: 11285298]
18. Crichton RR, Wilmet S, Legssyer R, Ward RJ. Molecular and cellular mechanisms of iron homeostasis and toxicity in mammalian cells. J Inorg Biochem. 2002; 91:9–18. [PubMed: 12121757]
19. Lee JC, Son YO, Choi KC, Jang YS. Hydrogen peroxide induces apoptosis of BJAB cells due to formation of hydroxyl radicals via intracellular iron-mediated Fenton chemistry in glucose oxidase-mediated oxidative stress. Mol Cells. 2006; 22:21–29. [PubMed: 16951546]
20. Repine JE, Fox RB, Berger EM. Hydrogen peroxide kills Staphylococcus aureus by reacting with staphylococcal iron to form hydroxyl radical. J Biol Chem. 1981; 256:7094–7096. [PubMed: 6265438]
21. Valko M, Morris H, Cronin MT. Metals, toxicity and oxidative stress. Curr Med Chem. 2005; 12:1161–1208. [PubMed: 15892631]
22. Achey P, Duryea H. Production of DNA strand breaks by the hydroxyl radical. Int J Radiat Biol Relat Stud Phys Chem Med. 1974; 25:595–601. [PubMed: 4547641]
23. Lai CS, Piette LH. Hydroxyl radical production involved in lipid peroxidation of rat liver microsomes. Biochem Biophys Res Commun. 1977; 78:51–59. [PubMed: 907691]
24. Rajpathak SN, Crandall JP, Wylie-Rosett J, et al. The role of iron in type 2 diabetes in humans. Biochim Biophys Acta. 2009; 1790:671–681. [PubMed: 18501198]
25. Canturk Z, Cetinarslan B, Tarkun I, Canturk NZ. Serum ferritin levels in poorly- and well-controlled diabetes mellitus. Endocr Res. 2003; 29:299–306. [PubMed: 14535631]
26. Van Campenhout A, Van Campenhout C, Lagrou AR, et al. Impact of diabetes mellitus on the relationships between iron-, inflammatory- and oxidative stress status. Diabetes Metab Res Rev. 2006; 22:444–454. [PubMed: 16506275]
27. Haap M, Fritsche A, Mensing HJ, Haring HU, Stumvoll M. Association of high serum ferritin concentration with glucose intolerance and insulin resistance in healthy people. Ann Intern Med. 2003; 139:869–871. [PubMed: 14623634]
28. Litwak KN, Cefalu WT, Wagner JD. Streptozotocin-induced diabetes mellitus in cynomolgus monkeys: changes in carbohydrate metabolism, skin glycation, and pancreatic islets. Lab Anim Sci. 1998; 48:172–178. [PubMed: 10090009]
29. Litwak KN, Cefalu WT, Wagner JD. Chronic hyperglycemia increases arterial low-density lipoprotein metabolism and atherosclerosis in cynomolgus monkeys. Metabolism. 1998; 47:947–954. [PubMed: 9711990]
30. Wagner JD, Zhang L, Greaves KA, Shadoan MK, Schwenke DC. Soy protein reduces the arterial low-density lipoprotein (LDL) concentration and delivery of LDL cholesterol to the arteries of diabetic and nondiabetic male cynomolgus monkeys. Metabolism. 2000; 49:1188–1196. [PubMed: 11016902]
31. Wagner JD, Shadoan MK, Zhang L, et al. Selective PPARα Agonist, CP-900691, Improves Plasma Lipids, Lipoproteins, and Glycemic Control in Diabetic Monkeys. J Pharmacol Exp Therap. 2010; 333:844–853. [PubMed: 20190014]
32. Katakam PV, Tulbert CD, Snipes JA, et al. Impaired insulin-induced vasodilation in small coronary arteries of Zucker obese rats is mediated by reactive oxygen species. Am J Physiol Heart Circ Physiol. 2005; 288:854–860.

33. Fink B, Laude K, McCann L, et al. Detection of intracellular superoxide formation in endothelial cells and intact tissues using dihydroethidium and an HPLC-based assay. Am J Physiol Cell Physiol. 2004; 287:C895–902. [PubMed: 15306539]
34. Shadoan MK, Zhang L, Wagner JD. Effects of hormone therapy on insulin signaling proteins in skeletal muscle of cynomolgus monkeys. Steroids. 2004; 69:313–318. [PubMed: 15219409]
35. Sullivan JL. Iron and arterial plaque: a modifiable risk factor for atherosclerosis. Biochim Biophys Acta. 2009; 1790:718–723. [PubMed: 18619522]
36. Goraya TY, Leibson CL, Palumbo PJ, et al. Coronary atherosclerosis in diabetes mellitus: a population-based autopsy study. J Am Coll Cardiol. 2002; 40:946–953. [PubMed: 12225721]
37. Fallow GD, Singh J. The prevalence, type and severity of cardiovascular disease in diabetic and non-diabetic patients: a matched-paired retrospective analysis using coronary angiography as the diagnostic tool. Mol Cell Biochem. 2004; 261:263–269. [PubMed: 15362512]
38. McGuire DK, Emanuelsson H, Granger CB, et al. Influence of diabetes mellitus on clinical outcomes across the spectrum of acute coronary syndromes. Findings from the GUSTO-IIb study. GUSTO IIb Investigators. Eur Heart J. 2000; 21:1750–1758. [PubMed: 11052839]
39. Gopaul NK, Anggard EE, Mallet AI, et al. Plasma 8-epi-PGF2 alpha levels are elevated in individuals with non-insulin dependent diabetes mellitus. FEBS Lett. 1995; 368:225–229. [PubMed: 7628610]
40. Nourooz-Zadeh J, Tajaddini-Sarmadi J, McCarthy S, Betteridge DJ, Wolff SP. Elevated levels of authentic plasma hydroperoxides in NIDDM. Diabetes. 1995; 44:1054–1058. [PubMed: 7657028]
41. Malle E, Marsche G, Arnhold J, Davies MJ. Modification of low-density lipoprotein by myeloperoxidase-derived oxidants and reagent hypochlorous acid. Biochim Biophys Acta. 2006; 1761:392–415. [PubMed: 16698314]
42. van Reyk DM, Brown AJ, Hult'en LM, Dean RT, Jessup W. Oxysterols in biological systems: sources, metabolism and pathophysiological relevance. Redox Rep. 2006; 11:255–262. [PubMed: 17207307]
43. Greenbaum CJ, Anderson AM, Dolan LM, et al. Preservation of beta-cell function in autoantibody-positive youth with diabetes. Diabetes Care. 2009; 32:1839–1844. [PubMed: 19587365]
44. Wagner JD, Cline JM, Shadoan MK, et al. Naturally occurring and experimental diabetes in cynomolgus monkeys: A comparison of carbohydrate and lipid metabolism and islet pathology. Toxicol Pathol. 2001; 29:142–148. [PubMed: 11215678]
45. Pacher P, Liaudet L, Soriano FG, et al. The role of poly(ADP-ribose) polymerase activation in the development of myocardial and endothelial dysfunction in diabetes. Diabetes. 2002; 51:514–521. [PubMed: 11812763]
46. Matsuoka T, Wada J, Hashimoto I, et al. Gene delivery of Tim44 reduces mitochondrial superoxide production and ameliorates neointimal proliferation of injured carotid artery in diabetic rats. Diabetes. 2005; 54:2882–2890. [PubMed: 16186389]
47. Basta G, Lazzerini G, Del Turco S, et al. At least 2 distinct pathways generating reactive oxygen species mediate vascular cell adhesion molecule-1 induction by advanced glycation end products. Arterioscler Thromb Vasc Biol. 2005; 25:1401–1407. [PubMed: 15845907]
48. Guzik TJ, Mussa S, Gastaldi D, et al. Mechanisms of increased vascular superoxide production in human diabetes mellitus: role of NAD(P)H oxidase and endothelial nitric oxide synthase. Circulation. 2002; 105:1656–1662. [PubMed: 11940543]
49. Wautier JL, Wautier MP, Schmidt AM, et al. Advanced glycation end products (AGEs) on the surface of diabetic erythrocytes bind to the vessel wall via a specific receptor inducing oxidant stress in the vasculature: a link between surface-associated AGEs and diabetic complications. Proc Nat'l Acad Sci (USA). 1994; 91:7742–7746.
50. Cappellini MD, Musallam KM, Taher AT. Overview of iron chelation therapy with desferrioxamine and deferiprone. Hemoglobin. 2009; 33(Suppl 1):S58–69. [PubMed: 20001633]
51. Minqin R, Rajendran R, Pan N, et al. The iron chelator desferrioxamine inhibits atherosclerotic lesion development and decreases lesion iron concentrations in the cholesterol-fed rabbit. Free Radic Biol Med. 2005; 38:1206–11. [PubMed: 15808418]
52. Zhang WJ, Wei H, Frei B. The iron chelator, desferrioxamine, reduces inflammation and atherosclerotic lesion development in experimental mice. Exp Biol Med. 2010; 235:633–641.

53. Dongiovanni P, Valenti L, Fracanzani AL, et al. Iron depletion by deferoxamine up-regulates glucose uptake and insulin signaling in hepatoma cells and in rat liver. Am J Pathol. 2008; 172:738–747. [PubMed: 18245813]

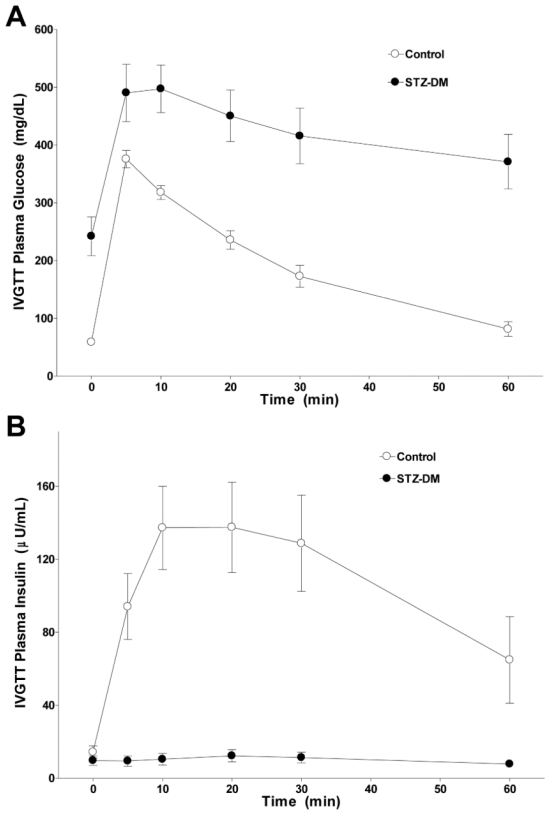

Figure 1. Effect of streptozotocin administration on β-cell responsiveness

Intravenous glucose tolerance tests were performed in both control monkeys (open circles) and STZ-DM monkeys (closed circles) seven days after diabetes induction as described in Methods. Values and vertical bars are means ± SEM (n = 10 animals per group) for plasma glucose (Panel A) and insulin (Panel B) concentrations measured at the indicated times after intervenous glucose bolus (750 mg/kg body wt) administration.

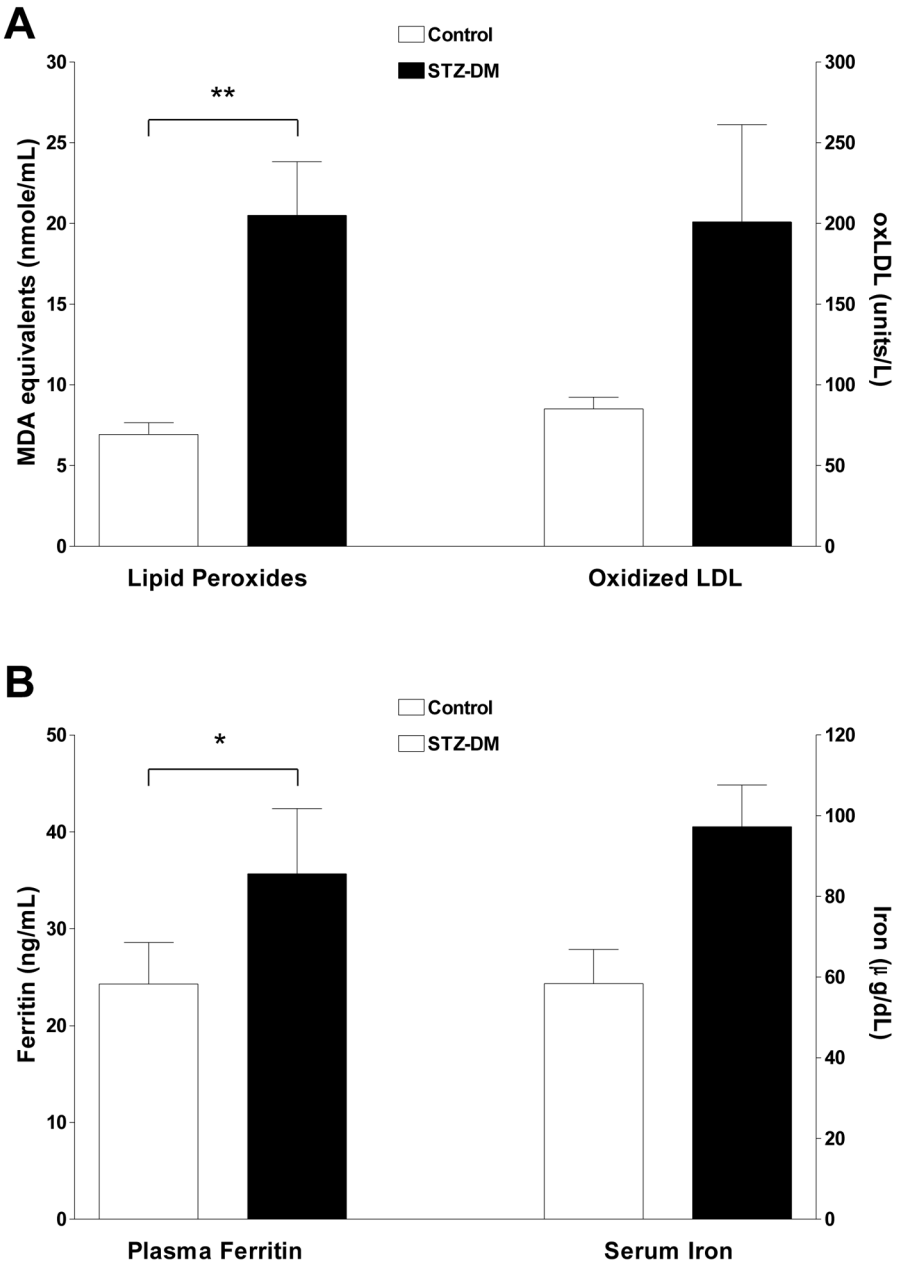

Figure 2. Plasma lipid peroxides, oxLDL, ferritin and iron levels in control and streptozotocin-treated monkeys

Fasting blood samples were obtained from control and streptozotocin-treated monkeys four weeks after diabetes induction and assessed for lipid peroxides, oxLDL, ferritin and iron levels as outlined in Methods. Panel A: data are the mean ± SEM for plasma lipid peroxides and oxLDL for control (white bars; n=10) and STZ-DM monkeys (black bars; n=10). Plasma lipid peroxides, quantified as thiobarbituric-acid reactive substances, are expressed as malondialdehyde equivalents (nmol/mL) (** = P<0.01, adjusted for baseline lipid peroxides). Plasma oxLDL is expressed as arbitrary units/L (T-test p=0.08, adjusted for baseline oxLDL). Panel B: data are the mean ± SEM for plasma ferritin and serum iron concentrations for control (white bars; n = 10) and STZ-DM monkeys (black bars; n = 10).

Plasma ferritin is expressed as ng/mL (* = $P < 0.05$, adjusted for baseline ferritin levels).
Serum iron is expressed as ug/dL (T-test p=0.08, adjusted for baseline iron levels).

Figure 3A

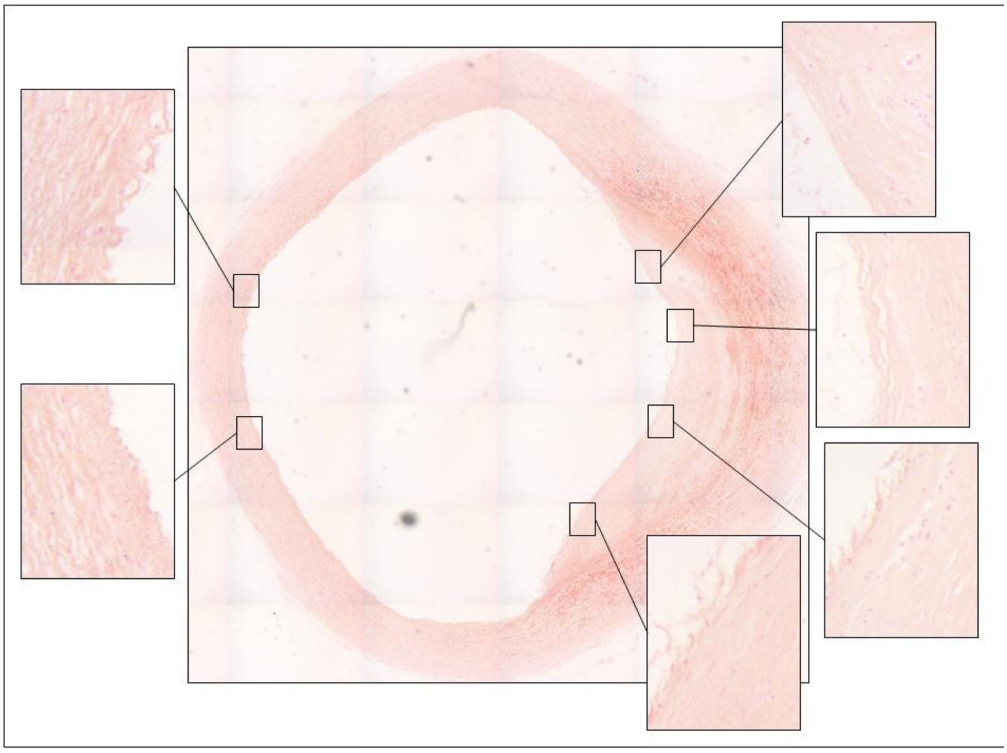

A. Aorta from control monkey

Figure 3B

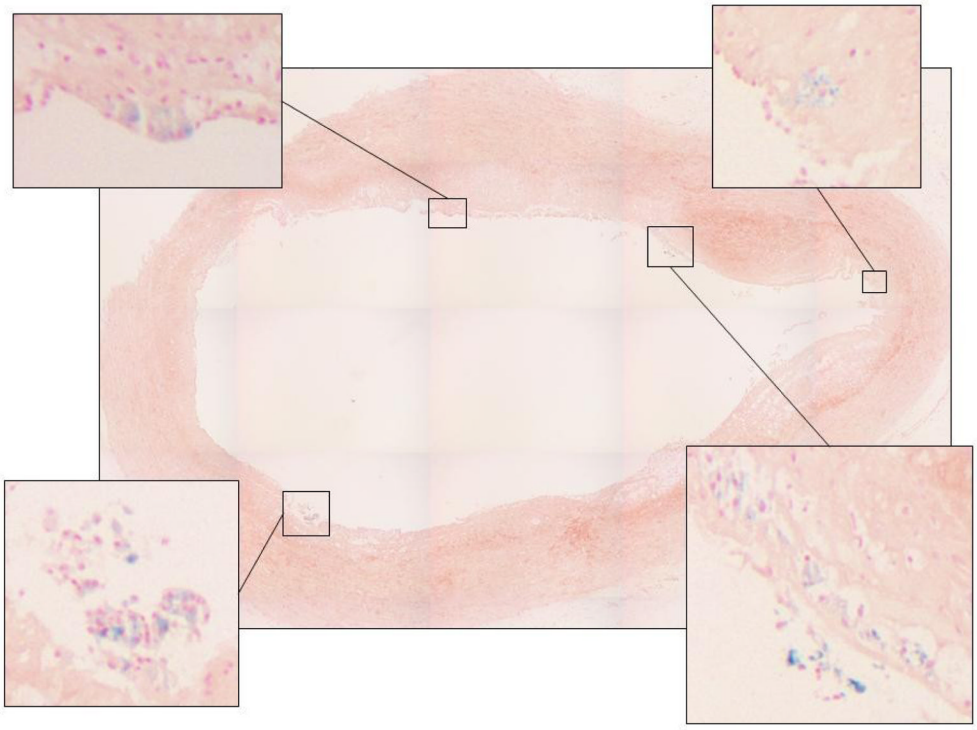

B. Aorta from STZ-DM monkey

Figure 3. Iron deposition in thoracic aortas from control and streptozotocin-treated monkeys

Cross sections of thoracic aorta tissue were fixed for immunohistochemistry and stained with Perl's stain for ferric iron (Fe^{3+}) as described in Methods. Panel A: aortic cross sections from control monkeys. Panel B: aortic cross sections from STZ-DM monkeys. Blue color indicates areas of iron staining. Inset pictures represent areas of staining that were expanded.

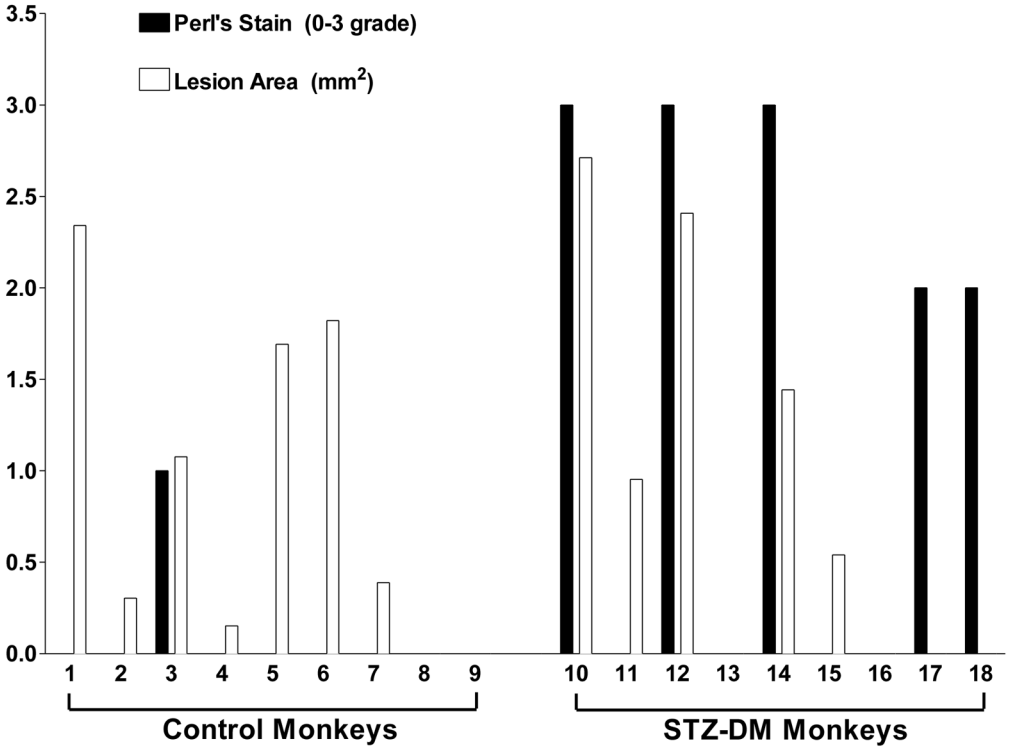

Figure 4. Atherosclerotic lesion area and iron staining in thoracic aortas from control and STZ-DM monkeys

Cross sections of aorta tissue were fixed for immunohistochemistry and stained with Perl's stain for ferric iron (Fe^{3+}) as described in Methods. Morphometric analysis was used to determine atherosclerotic lesion area (white bars). Perl's stain for Fe^{3+} (black bars) was quantified by assigning a grade of 0, 1, 2, or 3 based on presence or absence of blue staining as well as the number of stained regions within a section.

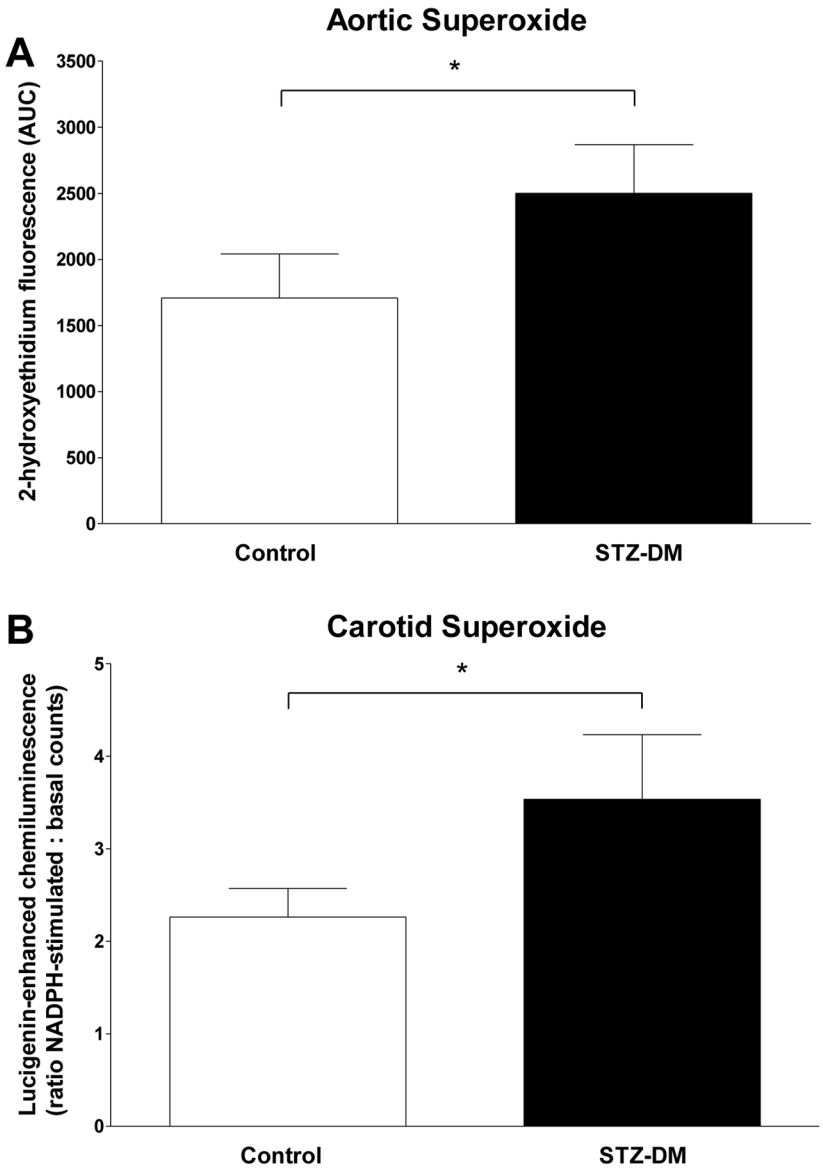

Figure 5. Arterial superoxide levels in control and streptozotocin-treated monkeys

Segments of carotid and aortic arteries were assessed for superoxide levels as outlined in Methods. Panel A: data are the mean ± SEM for superoxide anion-induced 2-hydroxyethidium fluorescence in aortic segments isolated from control (white bars; $n = 9$) and STZ-DM monkeys (black bars; $n = 9$). Arterial rings were incubated in dihydroethidine and subjected to HPLC separation. Formation of 2-hydroxyethidium in the presence of superoxide anion was quantified by fluorescence area-under-the-curve. Panel B: data are the mean ± SEM for the ratio of NADPH-stimulated to basal chemiluminescence in carotid arteries isolated from control (white bars; $n = 9$) and STZ-DM monkeys (black bars; $n = 9$). Luminescence is produced by the reaction of lucigenin with superoxide anion in the presence of NADPH. (* = $P < 0.05$).

Table 1

Effect of hyperglycemia on plasma glycemic indices in control and STZ-DM monkeys[a]

		Control	STZ-DM	p-value
Glucose (mg/dL)	Baseline	58 ± 1.1	63 ± 3.3	0.13
	Study End	54 ± 3	291 ± 52	< 0.001
Insulin (IU/L)	Baseline	14 ± 2.7	16 ± 2.1	0.54
	Study End	17.3 ± 3.9	8.8 ± 2.5	< 0.05
Fructosamine (μmol/L)	Baseline	192 ± 10	186 ± 13	0.72
	Study End	193 ± 10	260 ± 19	< 0.05
HbA_{1c} (%)	Baseline	4.4 ± 0.17	4.5 ± 0.16	0.44
	Study End	3.9 ± 0.12	6.8 ± 0.36	< 0.001
C-peptide (pmol/L)	Baseline	194 ± 23.5	224 ± 26.3	0.42
	Study End	250 ± 43.9	173 ± 51.7	0.05

[a]Fasting blood samples were obtained from control and streptozotocin-treated monkeys four weeks after diabetes induction. Data are presented as the mean ± SEM (n = 10 animals per group) together with respective ANCOVA p-values for study end parameter. Baseline parameters are assessed by students t-test.

Table 2

Effect of hyperglycemia on plasma and artery lipids in control and STZ-DM monkeys[a]

	Control (n=10)	STZ-DM (n=10)	p-value
Plasma lipids			
Total cholesterol (mg/dl)	233 ± 25	270 ± 32	0.91
ApoB cholesterol (mg/dl)	189 ± 29	227 ± 35	0.94
HDL cholesterol (mg/dl)	45 ± 5	43 ± 5	0.74
Triglycerides (mg/dl)	32 ± 4	152 ± 58	<0.05
Free fatty acids (mEq/l)	0.68 ± 0.10	0.80 ± 0.16	0.72
Carotid artery lipids			
Total cholesterol (μg/mg protein)	10.6 ± 3.2	14.2 ± 6.5	0.63
Free cholesterol (μg/mg protein)	5.9 ± 1.0	6.4 ± 2.4	0.85
Cholesterol ester (μg/mg protein)	5.5 ± 2.2	8.0 ± 4.1	0.53
Lipid peroxides (nmol/mg)	5.06 ± 1.24	4.73 ± 1.72	0.58
Aortic intimal area (mm2)	0.86 ± 0.30	0.83 ± 0.33	0.94

[a]Fasting blood samples and carotid artery lipids were obtained from control and streptozotocin-treated monkeys four weeks after diabetes induction. Aortic intimal area was determined by computer morphometric analysis. Data are presented as the mean ± SEM (n = 10 animals per group) together with respective T-test or ANCOVA p-values.

Table 3

Antioxidant enzyme levels in aortas from control and STZ-DM monkeys[a]

	Control	STZ-DM
EcSOD	2.84 ± 0.31	2.52 ± 0.15
MnSOD	4.09 ± 0.85	4.49 ± 0.90
Cu/ZnSOD	0.41 ± 0.05	0.38 ± 0.05
Catalase	0.065 ± 0.011	0.067 ± 0.010
Heme Oxygenase-1	0.028 ± 0.002	0.030 ± 0.004

[a]Aortic tissue was frozen in liquid nitrogen, and protein fractions containing the SODs, catalase, and heme oxygenase-1 were isolated and subject to gel electrophoresis and immunoblotting as outlined in Methods. Membranes were developed using an ECL-plus detection reagent and quantified by expressing their respective densities as arbitrary units normalized to that of β-actin bands as outlined in Methods. Values are means ± SEM (n = 10 animals per group).